# Frequency-Based Relationship of Electrowetting and Dielectrophoretic Liquid Microactuation

T. B. Jones*

*Department of Electrical & Computer Engineering, University of Rochester, Rochester, New York 14627*

Jesse David Fowler

*Mechanical and Aerospace Engineering Department, University of California at Los Angeles, Los Angeles, California 90095*

Young Soo Chang

*Thermal Flow Control Research Center, Korea Institute of Science and Technology, Seoul 136-791 (Korea)*

Chang-Jin Kim

*Mechanical and Aerospace Engineering Department, University of California at Los Angeles, Los Angeles, California 90095*

*Received May 2, 2003. In Final Form: June 17, 2003*

Electrowetting and dielectrophoretic actuation are potentially important microfluidic mechanisms for the transport, dispensing, and manipulation of liquid using simple electrode structures patterned on a substrate. These two mechanisms are, respectively, the low- and high-frequency limits of the electromechanical response of an aqueous liquid to an electric field. The Maxwell stress tensor and an RC circuit model are used to develop a simple predictive model for these electromechanics. The model is tested by measuring electric-field-induced pressure changes within an aqueous droplet trapped between two parallel, disk-shaped electrodes immersed in a bath of immiscible, insulating oil. The experiment is an adaptation of Quincke's original bubble method for measuring the dielectric constant of a liquid. For AC voltages lower than ∼100 V-rms, the pressure data largely conform to the square-law predictions of the model. At higher voltages, this square-law behavior is no longer evident, a result consistent with the well-known contact angle saturation effect. Pressure data obtained with DC electric fields are not consistent with either the lowest frequency data (10 Hz) or with the model.

## Introduction

Electric-field-based microfluidic schemes offer great promise in the laboratory on a chip and other $\mu$TAS (micro total analysis system) technologies. Using microfabricated electrodes and controlled application of AC or DC voltage, electrical body forces can manipulate and control nanoliter liquid masses, dispense picoliter droplets, and perform mixing and separation operations without discrete pumps or valves. Of growing interest among these are electrowetting on dielectric (EWOD) and dielectrophoretic (DEP) schemes, which share the attractive attributes of very high actuation speed and relative geometric simplicity. EWOD-based microfluidic systems usually confine liquid between a dielectric-coated electrode array patterned on a substrate and a transparent, dielectric-coated cover electrode.[1,2] Because DC or low-frequency AC voltage in the range of 25−200 V is usually employed, the electric field does not penetrate the liquid. For this reason, Joule heating is not significant and conductive liquids, including aqueous salt solutions, can be actuated.[3] DEP actuation utilizes even simpler, coplanar electrode structures, also dielectric coated, patterned on an open substrate. Usually, higher frequency AC voltage (∼10−200 kHz) in the range of ∼200−600 V is used.[4] Rapid DEP-mediated dispensing of large numbers of droplets in the ∼50 pL size range[5] and a voltage-controlled array mixer[6] have been demonstrated. Heating, which imposes an upper limit on the conductivity of liquids actuated by DEP, can be reduced if the electrodes are fabricated on an insulation-clad, metal substrate, which serves as a heat sink.[7]

The advantages of combining the simpler, open geometry and subnanoliter droplet dispensing capabilities of DEP microactuation with the lower frequency require-

* To whom correspondence should be addressed. E-mail: jones@ece.rochester.edu.

(1) Lee, J.; Moon, H.; Fowler, J.; Schoellhammer, T.; Kim, C.-J. Electrowetting and electrowetting-on-dielectric for microscale liquid handling. *Sens. Actuators* **2002**, *A95*, 259−268.

(2) Pollack, M. G.; Fair, R. B.; Shenderov, A. D. Electrowetting-based actuation of liquid droplets for microfluidic actuation. *Appl. Phys. Lett.* **2000**, *77*, 1725−1726.

(3) Moon, H.; Cho, S. K.; Garrell, R. L.; Kim, C.-J. Low voltage electrowetting-on-dielectric. *J. Appl. Phys.* **2002**, *92*, 4080−4087.

(4) Jones, T. B.; Gunji, M.; Washizu, M. Dielectrophoretic liquid actuation and nanodroplet formation. *J. Appl. Phys.* **2001**, *89*, 1441−1448.

(5) Ahmed, R.; Hsu, D.; Bailey, C.; Jones, T. B. Dispensing picoliter droplets using DEP micro-actuation. Microchannels and Minichannels Conference (ASME), Rochester, NY, April, 2003.

(6) Gunji, M.; Jones, T. B.; Washizu, M. DEP-driven simultaneous 2 × 2 droplet array mixer. *$\mu$TAS 2002 Proceedings* **2002**, *2*, 721−723.

(7) Gunji, M.; Washizu, M. Liquid DEP droplet actuator and mixer on a heat-conducting substrate. Annual IEEE/IAS Conference, Little Rock, AR, June, 2003.

10.1021/la0347511 CCC: $25.00 
Published on Web 07/26/2003

ments and the conductive liquid handling capabilities of EWOD are obvious. The motivation for the present work, therefore, is to explore the relationship between these two mechanisms in the hope that their attractive attributes can be effectively combined in a new microfluidic scheme. In this paper, we present a simple, frequency-dependent electromechanical force model to show that the EWOD and DEP effects are, respectively, the high- and low-frequency limits of what amounts to the same basic response of a liquid to an electric field. These limits, again respectively, correspond to the cases of conducting and insulating liquids. The theory is accompanied by experimental measurements of the electromechanical force, obtained using an adaptation of the bubble technique used over 120 years ago by Quincke.[8,9] The experiments generally support the theoretical predictions of the model with respect to the frequency dependence; however, certain discrepancies revealed at the lowest frequencies and DC suggest other influences on the electromechanics of aqueous liquids. This work has implications in microfluidic control for the laboratory on a chip, namely, that the distinctive and advantageous attributes of both EWOD and DEP can be exploited in a single structure merely by adjusting frequency.

## Background

The electrical force acting on isotropic liquids is usually formulated in terms of the Korteweg−Helmholtz body force density.[10,11]

$$\bar{f}^{\,e} = \rho_f \bar{E} - \frac{1}{2}E^2\,\nabla\epsilon + \nabla\left[\frac{1}{2}E^2\,\frac{\partial\epsilon}{\partial\rho}\rho\right] \qquad (1)$$

where $E$ is the electric field, $\rho_f$ is the volume density of free electric charge, $\epsilon$ is the permittivity, and $\rho$ is the mass density of the liquid, which need not be homogeneous. Electrical force density formulations are not unique in classical continuum electrodynamics;[12] eq 1 is selected for its advantages in certain problems involving homogeneous, incompressible liquids. We assume the volume charge density in the liquid is zero, that is, $\rho_f = 0$, but accept the possibility of surface charge. Furthermore, for a homogeneous and incompressible liquid, the third, pressure-like term in eq 1, that is, electrostriction, has no influence on the hydrostatics and can be ignored.[13] As a consequence, only forces acting at free, liquid interfaces contribute to translational motion of the liquid. These forces are (i) the ponderomotive force term proportional to $\nabla\epsilon$[14] and (ii) the force exerted by the electric field on free charge induced at the surface. In our analysis of the Quincke bubble method, we take advantage of the location of these *apparent* body forces at interfaces.

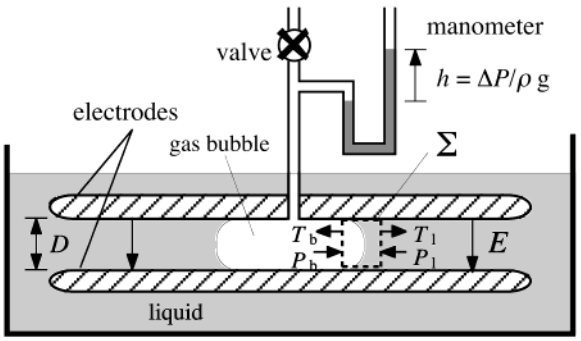


**Figure 1.** Quincke's bubble technique for measuring the apparent pressure drop $\Delta P_e$ across a gas/liquid interface induced by a uniform electric field $E$ parallel to the interface. An insulating dielectric liquid was used (dielectric constant $= \kappa_l$), and the gas was dry air ($\kappa_b \approx 1$). The parallel electrodes were uncoated. The closed surface $\Sigma$ is used to define the equilibrium condition, eq 4.

The form of the Maxwell stress tensor consistent with the body force expression of eq 1 is[11]

$$T^{e}_{mn} = \epsilon E_m E_n - \delta_{mn}\frac{1}{2}[\epsilon - (\partial\epsilon/\partial\rho)\rho]E_k E_k \qquad (2)$$

In eq 2, the Einstein summation convention is used and $\delta_{mn}$ is the Kronecker delta function. The stress tensor is convenient for determining the *net* force on an object. For example, the net, $z$-directed, translational force on a body inside a closed surface $\Sigma$ is

$$F^{e}_{z} = \oint_{\Sigma} T^{e}_{mn}\, n_n\, dA \qquad (3)$$

where $n_n$ is the unit normal on the $n$th face of $\Sigma$. The advantage of calculating net force using the stress tensor is that we may choose the surface of integration $\Sigma$ at our convenience, thereby often obviating the need to know details of the electric fringing field.[11] This advantage carries over to the case of EWOD and liquid DEP actuation, where, *if the only objective is to determine the net force of electrical origin*, it is unnecessary to deal with electric-field-induced changes of the liquid profile, including those attributed to the contact angle, along the solid/liquid contact line.[15]

**Quincke's Bubble Technique.** Quincke's basic apparatus for investigating the electromechanical forces exerted on insulating, dielectric liquids is depicted in Figure 1. A volume of gas is introduced through a tube at the center of two parallel, closely spaced, circular electrodes which are mounted horizontally and completely immersed in an insulating dielectric liquid of dielectric constant $\kappa_l$. The tube is next closed off so that the flat bubble trapped between the electrodes is in pressure communication only with the manometer tube. Pressure changes are then measured as a function of the voltage $V$ applied between the electrodes.

The Maxwell stress tensor may be used to predict this pressure change. Consider the interfacial equilibrium condition. If $P_b$, $T_b$ and $P_l$, $T_l$ are, respectively, the hydrostatic pressures and normal Maxwell surface stresses acting on the vertical faces of a closed surface $\Sigma$ enclosing a section of the interface, then

$$T_b - P_b = T_l - P_l - \Delta P_{cap} \qquad (4)$$

(8) Quincke, G. Electrische Untersuchungen. *Ann. Phys. Chem., 3rd Ser.* (*Leipzig*) **1883**, *255*, 705−782.
(9) Pickard, W. F. Electrical force effects in dielectric liquids. *Prog. Dielectr.* **1965**, *6*, 1−39.
(10) Landau., L. D.; Lifshitz, E. M. *Electrodynamics of continuous media*; Pergamon: Oxford, 1960; Section 15.
(11) Woodson, H. H.; Melcher, J. R. *Electromechanical dynamics, part I*: *Discrete systems*; Wiley: New York, 1968; Chapter 7.
(12) Melcher, J. R. A tutorial on induced electrohydrodynamic forces. MIT, unpublished, ca. 1968 (available by request from the authors).
(13) Rosenkilde, C. E. A dielectric fluid drop in an electric field. *Proc. Royal Soc.* (*London*) **1969**, *A312*, 473−494.
(14) The ponderomotive term of the Korteweg−Helmholtz body force density might seem to be nonphysical, as there is no obvious mechanism for a dipole force at a boundary when no electric field gradient exists; however, the proper usage of eq 1 is only to calculate the *total* force on a ponderable body by an appropriate volume integral or by a surface integral of the Maxwell stress tensor. Attaching physical significance to the point-by-point distribution of a body force formulation is not always meaningful and anyway unnecessary.
(15) Jones, T. B. On the relationship of dielectrophoresis and electrowetting. *Langmuir* **2002**, *18*, 4437−4443.

where $\Delta P_{cap}$ is the net capillary pressure contribution due to surface curvature in the absence of the electric field. If $\Delta P = P_b - P_l$ is the total hydrostatic pressure measured by the manometer, then the contribution to $\Delta P$ caused by the electrostatic force is $\Delta P_e = T_b - T_l$.[16] Equation 2, with the electrostriction term ignored, may be used to evaluate this pressure term.

$$\Delta P_e \approx (\kappa_l - \kappa_b)\epsilon_0 E^2/2 \tag{5}$$

where $\kappa_b$ and $\kappa_l$ are the dielectric constants of the gas bubble ($\kappa_b \approx 1$) and the liquid, respectively, $\epsilon_0 = 8.854 \times 10^{-12}$ F/m is the permittivity of free space, and $E$ is the uniform electric field between the electrodes and tangential to the vertical surfaces of $\Sigma$. Note that the electric-field-induced pressure change is positive because $\kappa_l > \kappa_b$. Equation 5 is accurate as long as the uniform electric field approximation, that is, $E = V/D$, is valid, where $D$ is the electrode spacing. For this to be so, $D$ must be small compared to the radius of the trapped bubble.

### Adaptation of Quincke's Method for Electrowetting

To investigate the relationship of EWOD and liquid DEP, we adapted Quincke's bubble method by coating both electrodes with thin layers of dielectric, replacing the trapped gas bubble with a droplet of aqueous liquid and using variable frequency AC voltage. To model this new experiment, eq 5 must be replaced by a different expression for the electromechanically induced pressure, one that accounts for the dielectric coatings and the frequency dependence of the electric field distribution. The gas bubble is replaced by a water droplet of dielectric constant $\kappa_w$ and electrical conductivity $\sigma_w$. For modeling purposes, assume identical dielectric layers of thickness $d \ll D$ and dielectric constant $\kappa_d$ cover each of the electrodes as shown in Figure 2a. According to the Korteweg–Helmholtz formulation for the force of electrical origin, that is, eq 1, the components that contribute to measurable pressure change act only at the liquid/air interface. The Maxwell stress tensor is used to evaluate $\Delta P_e$ by again locating the right and left vertical surfaces of $\Sigma$ far from the curved liquid/liquid interface to avoid distortion of the electric field. In Figure 2a, note the labeling used to signify different sections of $\Sigma$ representing nonzero contributions to the surface integral: 1, 2, and 3 within the water droplet and 4, 5, and 6 in the insulating liquid.

To determine the Maxwell stresses, expressions for the uniform, tangential electric fields at these sections of the surface, namely, $E_d$, $E_l$, $E'_d$, and $E_w$, are obtained using the simple RC circuit shown in Figure 2b. For convenience, the capacitance and conductance quantities are expressed per unit area.

$$c_d = \kappa_d\epsilon_0/d \qquad c_l = \kappa_l\epsilon_0/D \tag{6a}$$

$$c_w = \kappa_w\epsilon_0/D \qquad g_w = \sigma_w/D \tag{6b}$$

where $\sigma_w$ is electrical conductivity. The circuit model in Figure 2b ignores the double-layer capacitance at the liquid/metal interface. Such capacitance, while likely to be very large compared to $c_d$, is series-connected and thus may be safely ignored.[17] Let $V(t) = \mathrm{Re}[(\sqrt{2})Ve^{j\omega t}]$, where $\omega$ is the radian frequency and $V$ is the root-mean-square

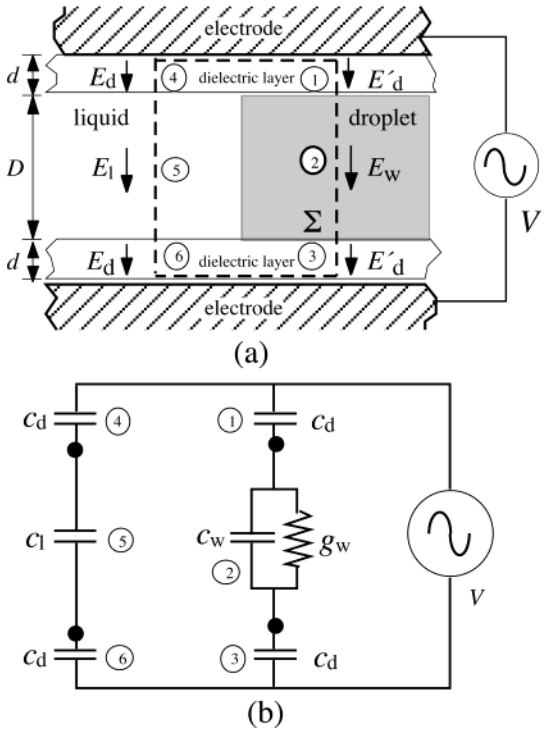


**Figure 2.** (a) Definition of the closed surface integral $\Sigma$ and associated area segments for Maxwell stress tensor based determination of the net electrically induced pressure drop $\Delta P_e$ measured in the modified Quincke apparatus using coated electrodes. (b) Circuit model for determining frequency-dependent voltage and electric field distributions.

(rms) magnitude of applied voltage. Then, the rms electric field magnitudes are

$$E_d = \frac{c_l}{2c_l + c_d} V/d \tag{7a}$$

$$E_l = \frac{c_d}{2c_l + c_d} V/D \tag{7b}$$

$$E'_d = \mathrm{Re}\left[\frac{j\omega c_w + g_w}{j\omega(2c_w + c_d) + 2g_w} V/d\right] \tag{7c}$$

$$E_w = \mathrm{Re}\left[\frac{j\omega c_d}{j\omega(2c_w + c_d) + 2g_w} V/D\right] \tag{7d}$$

The surface integral for the horizontal, $z$-directed component of the force of electrical origin consists of the sum of the six contributions defined in Figure 2a. Using eqs 2, 3, and 7a–d, the time-average force per unit length of the contact line is

$$\langle F^e_z \rangle = -\kappa_d\epsilon_0 {E_d}^2 d - \frac{\kappa_l\epsilon_0 {E_l}^2}{2} D + \kappa_d\epsilon_0 {E'_d}^2 d + \frac{\kappa_w\epsilon_0 {E_w}^2}{2} D \tag{8}$$

The measurable pressure change induced by the electric field is then

$$\Delta P_e = \langle F^e_z \rangle / D \tag{9}$$

(16) Derivation of the electromechanical pressure term $\Delta P_e$ is based on an energy argument and, as such, accounts completely for all electrical contributions to the measured pressure change. It is thus incorrect to include an additional term based on the change in the contact angle caused by the electric field because to do so would be double-counting.

(17) Shapiro, B.; Moon, H.; Garrell, R.; Kim, C.-J. Equilibrium behavior of sessile droplets under surface tension, applied external fields, and material variations. *J. Appl. Phys.* **2003**, *93*, 5794–5811.

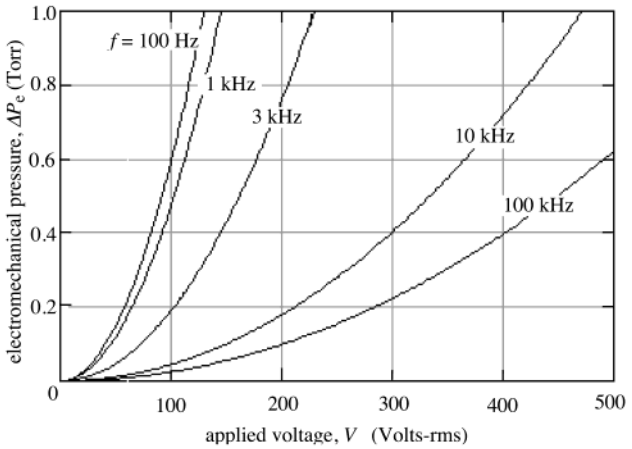


**Figure 3.** Predicted electromechanical pressure $\Delta P_e$, eq 9, versus voltage $V$ for the modified Quincke apparatus with coated electrodes at frequencies ranging from 100 Hz (the EWOD limit) to 100 kHz (the DEP limit). Insulating liquid: $\kappa_l = 2.1$. Water: $\sigma_w = 2 \times 10^{-4}$ S/m, $\kappa_w = 80$. Dielectric coating: $d = 0.75$ $\mu$m, $\kappa_d = 2.7$. Electrode spacing: $D = 1$ mm.

An easy way to test eq 9 is to consider its high- and low-frequency limits. Inspection of eqs 7c,d reveals a critical frequency at

$$\omega_c = \frac{2g_w}{2c_w + c_d} \tag{10}$$

For $\omega \ll \omega_c$, the water behaves like a perfectly conducting medium, that is, $E$ is zero in the water and the entire voltage drop is concentrated in the dielectric layer. On the other hand, when $\omega \gg \omega_c$, the water behaves like a dielectric and the voltage distribution is as it would be for capacitive voltage division. If it is assumed that $d \ll D$, then the limits of eq 9 are

$$\Delta P_e \approx \begin{cases} \dfrac{\kappa_d \epsilon_0 V^2}{4dD} & \omega \ll \omega_c \\ \dfrac{(\kappa_w - \kappa_l)\epsilon_0 V^2}{2D^2} & \omega \gg \omega_c \end{cases} \tag{11}$$

In eq 11, the $\omega \ll \omega_c$ limit is the well-known result from EWOD,[18] while the expression for $\omega \gg \omega_c$ is the same as eq 5 above. It is also evident that these expressions correspond to the perfectly conducting and perfectly insulating limits for the liquid, again respectively.[15]

Figure 3 plots calculated values of $\Delta P_e$ versus voltage $V$ for the following parameter set: $\kappa_l = 2.1$, $\sigma_w = 2 \times 10^{-4}$ S/m, $\kappa_w = 80$, $d = 0.75$ $\mu$m, $\kappa_d = 2.7$, and $D = 1$ mm. The frequencies used for the plot bracket the critical value, $\omega_c/2\pi = 1$ kHz. The model predicts that the magnitude of electromechanical pressure $\Delta P_e$ is much greater at lower frequencies, a result readily explained by the RC circuit model of Figure 2b. For $\omega \ll \omega_c$, the entire voltage drop occurs across the dielectric layers. In this case, electric field intensification near the contact line induces surface charge at the liquid/air interface, as pointed out by Kang.[19] But for the fact that water has a very high dielectric constant, $\kappa_w = 80 \gg \kappa_d \sim 2.7$, the differences between low and high frequencies would be even more dramatic.

(18) Welters, W. J. J.; Fokkink, L. G. J. Fast electrically switchable capillary effects. *Langmuir* **1998**, *14*, 1535−1538.

(19) Kang, K. H.; Kang, I. S.; Lee, C. M. Wetting tension due to Coulombic interaction in charge-related wetting phenomena. *Langmuir* **2002**, *18*, 10318−10322.

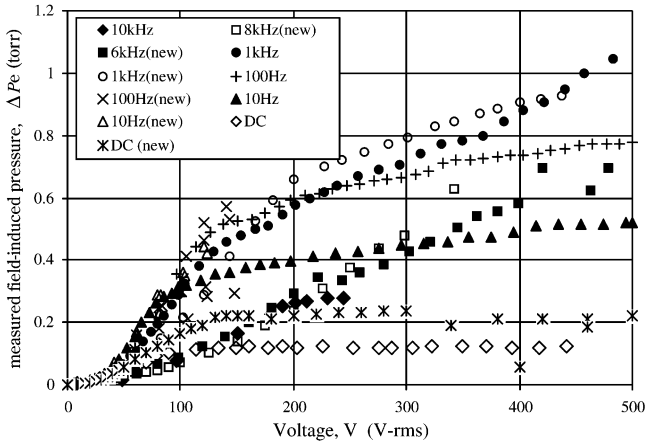


**Figure 4.** Experimental pressure data obtained with the modified Quincke apparatus for DC and AC voltages from 10 Hz to 10 kHz. The lower electrode (500 $\mu$m Si wafer) was coated with 1 $\mu$m of $SiO_2$ and 0.25 $\mu$m of Teflon-AF, and the upper electrode (ITO on glass) was coated by 0.25 $\mu$m of Teflon. The electrode spacing was fixed by glass spacers at $D = 1$ mm. The insulating liquid used was transformer oil with $\kappa_l = 2.1$. The droplet was deionized water. MKS Baratron and Omega differential pressure gauges were used to measure the pressure in the water droplet. Measurements made with the Omega transducer are designated "(new)" in the data key.

## Experiment

A modified Quincke apparatus was constructed to measure the frequency dependence of the electric surface traction $\Delta P_e$ for coated electrodes and water. The electrically grounded, lower electrode was made from a silicon wafer, coated first with 1 $\mu$m of thermally grown $SiO_2$ for electrical insulation and then with 0.25 $\mu$m of Teflon-AF to control the wetting. The upper electrode was made with a 1400 Å layer of ITO (indium tin oxide) deposited on borosilicate glass and then coated with 0.25 $\mu$m of Teflon, again for wetting control. The electrodes were held apart by 1 mm thick glass spacers, and the entire cell was immersed in a bath of GE 10-C transformer oil, which is immiscible with water. Pressure was measured with two electronic differential pressure gauges: an MKS Baratron (model no. 145BH-10), 10 Torr full-scale, capable of discriminating pressure differences down to ~0.0001 Torr; and an Omega (model no. PX154-001DI), 1.87 Torr full-scale, capable of discriminating pressure differences down to ~0.001 Torr. Data obtained with the Omega unit are designated "(new)".

Measurements were performed from DC to 10 kHz using DI (deionized) water. DI water was chosen primarily for convenience.[20] Because no strenuous effort was made with respect to its handling, we estimate the range of the water's electrical conductivity: $5 \times 10^{-5} < \sigma_w < 2 \times 10^{-4}$ S/m.

Figure 4 is a composite plot of all the data obtained with the apparatus, covering DC and variable frequency AC voltages up to ~500 V-rms. One can make several observations about these results. First, for DC and AC voltage at frequencies of 10, 100, and 1000 Hz, the pressure versus voltage data reveal an evident breakpoint near ~100 V-rms. Below this value, the voltage dependence is approximately square-law, $V^2$, while above it the dependence becomes much weaker. This behavior appears to be consistent with contact angle saturation. Second, the 100 Hz and 1 kHz data seem to diverge steadily from the 10 Hz data at voltages above ~150 V-rms. Third, for the higher frequencies, $f \geq 6$ kHz, the measured electromechanical pressure drops off, as predicted by the theory presented above and displayed in

(20) Experimentation with ionic salt solutions (e.g., KCl) would introduce the possibility of adjusting the electrical conductivity in a controlled fashion. Such experiments are ultimately of great interest, and we plan to pursue them. But working with salt solutions adds the major complication of having to worry about electrolysis and salt buildup on the coated electrodes, which could damage the dielectric coatings. For the purpose of showing the frequency-dependent relationship of DEP and EWOD, we elected to fix the conductivity and vary the frequency.

Figure 3. Fourth, the pressure data obtained with DC are dramatically lower than the $f = 10$ Hz results.

## Discussion

Contact angle saturation, which limits the minimum value of the observable contact angle for sessile droplets as voltage is increased, has been found by others to correspond rather well to a limit reported for the EWOD-induced height-of-rise of an aqueous liquid in a capillary tube.[18] Shapiro et al. have recently proposed a rather general model for the phenomenon.[17] This behavior may be linked to electric field intensification at the contact line; according to this hypothesis, the field reaches some critical threshold as the wetting angle of a conducting liquid becomes smaller with increasing voltage. There is evidence of corona discharge emanating from the edge of the contact line[21] and also an interfacial electrohydrodynamic instability that ejects large numbers of very small droplets.[22,23] Because ion and droplet ejection mechanisms involve momentum transfer, both are capable of (i) limiting the contact angle effect and (ii) interfering with the electromechanical response of liquid at a dielectric-coated electrode.

The DC voltage at which saturation occurs can be estimated by substituting observed values for the saturation angle $\theta_{sat}$ into the equation of Berge.[24] Some work on contact angle phenomena in water/oil/solid systems has been reported,[25] but the manifestations of saturation in such systems are not well-known. The data in Figure 4 strongly suggest the onset of saturation behavior at ~100 V-rms, a value consistent with those reported by others. This saturation exhibits a dependence on the frequency, a result one might anticipate because the accumulation of electric charge at the water/oil interface near the contact line is expected to diminish rapidly once $\omega > \omega_c$.

**Response below the Saturation Limit.** Figure 5 plots the pressure data up to 120 V-rms, along with theoretical curves calculated using eq 9. By focusing on this lower voltage range, we effectively avoid the influence of contact angle saturation, a phenomenon which neither our electromechanical model nor any other yet available accounts for in a satisfactory fashion. To compare the experiment to the predictive relationship, eq 9, the multiple layers of dielectric (viz., the $SiO_2$ and Teflon coatings) are represented by identical, homogeneous layers covering each electrode with $d = 0.75$ microns and effective dielectric constant $\kappa_d = 2.7$. This approximation does not compromise the accuracy of the predicted frequency dependence. Using the parameters of the experimental apparatus in eqs 6a,b and 10 with water conductivity $\sigma_w = 2 \times 10^{-4}$ S/m, we estimate the critical frequency ($\omega_c/2\pi$) to be ~1 kHz. The major uncertainty in this estimate arises from the conductivity of the DI water used in the experiments. Except for DC, the data in Figure 5 conform fairly well to the predictions of the model for $V \leq$ ~100 V-rms. For example, despite some scatter, the 10 and 100 Hz data all group together somewhat below the theoretical

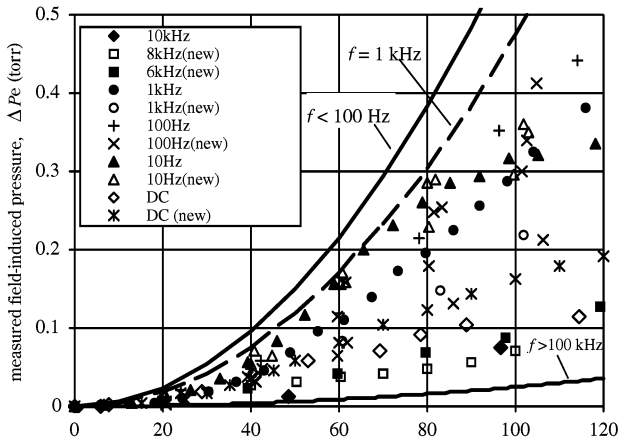


**Figure 5.** Replot of pressure data from Figure 4 for voltages up to 120 V-rms. At these lower voltages, the effects of contact angle saturation are minimized, facilitating comparison of the data to the predictive electromechanical theory, eq 9. Note that if the scatter associated with certain $f = 100$ Hz data is ignored, the frequency dependence of $\Delta P_e$ is largely confirmed for frequencies of ≥10 Hz. On the other hand, the DC data are not consistent with the model. The theoretical curves are calculated using eq 9 for the following parameters. Insulating liquid: $\kappa_l = 2.1$. Water: $\sigma_w = 2 \times 10^{-4}$ S/m, $\kappa_w = 80$. Dielectric coating: $d = 0.75$ $\mu$m, $\kappa_d = 2.7$. Electrode spacing: $D = 1$ mm.

low-frequency curve. The 1 kHz data appear to drop off a bit from this grouping, and this trend, entirely consistent with the model, continues at the higher frequencies, 6−10 kHz. The 10 kHz data lie somewhat above the high-frequency theoretical curve, presumably because still higher frequencies, not possible with our equipment, are required to approach the DEP limit. In general, all the AC data exhibit reasonably good qualitative and quantitative agreement with the model.

On the other hand, the DC data do not conform well to either the AC data or the theory. The model predicts that for a DC electric field, the pressure should be maximized, whereas in fact the pressure data are considerably lower than the results at 10 Hz. A possible explanation for this anomalous behavior is that DC electric fields, unlike AC, provide no time-varying force component to help overcome wetting-related stiction effects. Further, we cannot rule out the possibility that electrolysis has an influence on the DC behavior. We saw no visual evidence of bubbles; however, our experimental setup did not permit microscopic observation of the water−surface interface.

## Conclusion

We have presented a simple electromechanical theory to predict the electromechanical response of a conductive, dielectric liquid to AC electric fields. The force is calculated using the Maxwell stress tensor; an RC circuit is used to predict the frequency dependence of the electric field distribution. We use the model to calculate the measurable pressure change in a modification of Quincke's original apparatus, where a droplet of aqueous liquid replaces the gas bubble and both parallel electrodes are coated with thin insulating dielectric layers. The electric-field-induced pressure change within the droplet $\Delta P_e$ is measured as a function of voltage for frequencies from DC to 10 kHz. The low- and high-frequency limits of the resulting predictive equation are identical to previously published results for the cases of perfectly conductive and perfectly insulative dielectric liquids, respectively. The perfectly conducting limit corresponds to the case of the EWOD phenomenon, while the insulating case is the same as Quincke's original experiment. Using the Maxwell stress

(21) Vallet, M.; Vallade, M.; Berge, B. Limiting phenomena for the spreading of water on polymer films by electrowetting. *Eur. Phys. J.* **1999**, B11, 583−591.

(22) Vallet, M.; Berge, B.; Vovelle, L. Electrowetting of water and aqueous solutions on poly(ethylene terephthalate) insulating films. *Polymer* **1996**, *37*, 2465−2470.

(23) Mugele, F.; Herminghaus, S. Electrostatic stabilization of fluid microstructures. *Appl. Phys. Lett.* **2002**, *81*, 2303−2305.

(24) Berge, B. Électrocapillarité et mouillage de films isolants par l'eau. *C. R. Acad. Sci., Ser. II* **1993**, *317*, 157−163.

(25) Janocka, B.; Bauser, H.; Oehr, C.; Brunner, H.; Göpel, W. Competitive electrowetting of polymer surfaces by water and decane. *Langmuir* **2000**, *16*, 3349−3354.

tensor method avoids any need for information about the distortion of the electric field near the interface, the distribution of induced electric surface charge, and the contact angle the liquid makes with the coated electrodes. At low frequencies, the force, measured as a pressure difference, is due to the locally intense electric field acting on free induced charge at the liquid/air interface. As frequency is increased, the force makes a steady transition from that situation to a case where the (ponderomotive) force on dipoles dominates. In homogeneous liquids, the Korteweg−Helmholtz formulation of the force density, that is, eq 1, places the apparent force at the interface.

To test the theoretical model, we limit consideration to the experimental data in the range $0 < V \leq 120$ V-rms. Doing so avoids the complication of contact angle saturation, which cannot be accounted for readily in the model. We find that the low-voltage experimental data for $f \geq 10$ Hz conform to the predictions of the model. Within limits imposed by uncertainty in some experimental parameters, the 10 Hz, 100 Hz, and 1 kHz data correlate reasonably well to the low-frequency (EWOD) limit. For frequencies above ~1 kHz, $\Delta P_e$ is reduced just as predicted, and the 10 kHz data approach the high-frequency limit.

At the lower voltages, only the DC data seem to deviate from the theory. Whereas the theory predicts that the electromechanical force should be maximized in the DC limit, the pressure drops measured with applied DC voltage are much lower than the 10 and 100 Hz data. At the present time, there is no satisfactory explanation for this anomaly. A possible explanation is contact angle hysteresis. The way such nonconservative behavior might influence the time-averaged pressure drops we measure in the Quincke apparatus is not immediately obvious, but Blake et al. present a very interesting argument for their dynamic system that might be adaptable.[26] There also is seen to be a fairly dramatic effect of frequency on the saturation effect itself; the strongest evidence of this phenomenon is seen at DC and 10 Hz, with a threshold of ~100 V-rms, while at 1 kHz and above, the onset is more gradual. This frequency dependence could be related to the fact that the accumulation of free surface charge diminishes as frequency is increased. Whatever its explanation, the DC behavior is important and merits further study because of the practical advantages of DC-voltage-actuated microfluidics in $\mu$TAS technologies. One approach now under consideration is to perform new measurements using DC voltage combined with AC in the frequency range from 1 to 10 Hz.

**Acknowledgment.** All experimental measurements were performed in C.-J. Kim's laboratory at UCLA. M. Washizu (Tokyo University), T. Blake (Eastman Kodak Ltd.), and K.-H. Kang (Pohang University of Science & Technology, Korea) have provided useful comments to T.B.J. on the modeling of electrowetting and dielectrophoresis phenomena. The authors acknowledge contributions of Sandia National Laboratories, Livermore, CA, to this work in the form of a summer internship for J.D.F. and the use of laboratories and equipment in support of the early stages of this research. This work is supported by grants from the National Institutes of Health, the Center for Future Health of the University of Rochester, the Infotonics Technology Center, Inc. (NASA Grant No. NAG3-2744), the NSF IGERT (Materials Creation Training Program Fellowship to J.D.F.), and the DARPA BioFlips program.

LA0347511

(26) Blake, T. D.; Clarke, A.; Stattersfield, E. H. An investigation of electrostatic assist in dynamic wetting. *Langmuir* **2000**, *16*, 2928−2935.